



Contents lists available at ScienceDirect

## Journal of Sound and Vibration

journal homepage: [www.elsevier.com/locate/jsvi](http://www.elsevier.com/locate/jsvi)

## Approximations for motion of the oscillators with a non-negative real-power restoring force

Zvonko Rakaric, Ivana Kovacic \*

Department of Mechanics, Faculty of Technical Sciences, University of Novi Sad, 21215 Novi Sad, Serbia

## ARTICLE INFO

## Article history:

Received 5 May 2010

Received in revised form

4 August 2010

Accepted 4 August 2010

Handling Editor: M.P. Cartmell

## ABSTRACT

Oscillators with a non-negative real-power restoring force are considered in this paper. This type of restoring force is related to systems with a quasi-zero stiffness characteristic or those in which the restoring force is purely nonlinear in nature. Examples of these types of restoring force are grounded in real physical and engineering systems. Periodic motion of such conservative oscillators is described first in a novel way by means of the elliptic function the parameters of which are obtained from the energy conservation law and Hamilton's variational principle. Then, the approach is extended to non-conservative oscillators by adjusting the elliptic Krylov–Bogoliubov method. The methods proposed for the conservative and non-conservative systems under consideration have wider applications than the existing one with respect to the power of the restoring force. Several examples, the majority of which are so far unsolved, are given to illustrate the methods proposed and to demonstrate their generality, which permits unforeseen solutions for motion, containing higher harmonics and assuring consistent accuracy regardless of the value of the power of the restoring force. The results obtained are compared with numerical results and have excellent accuracy.

© 2010 Elsevier Ltd. All rights reserved.

### 1. Introduction

In this paper single-degree-of-freedom autonomous oscillators with a non-negative real-power restoring force are considered

$$M\ddot{x} + F(x, \dot{x}) + C \operatorname{sgn}(x)|x|^\alpha = 0, \quad (1)$$

where  $M$  is a mass,  $x$  is displacement, dots stand for the differentiation with respect to time  $t$ ,  $C$  is the coefficient of the restoring force and  $\alpha$  is its power that can be any non-negative real number. The function  $F$  stands for non-conservative forces which, in general, depend on the displacement and velocity. When  $F=0$ , the oscillators are conservative. The initial conditions are prescribed as

$$x(0) = X_0, \quad \dot{x}(0) = 0, \quad (2)$$

where  $X_0$  is a positive real constant.

The non-negative real-power restoring force given by the last term in Eq. (1) can originate from two types of systems. The first type relates to the originally multi-term restoring force tuned to have a quasi-zero stiffness characteristic, which

\* Corresponding author. Tel.: +381 214852241; fax +381 21450207.  
E-mail address: [ivanakov@uns.ac.rs](mailto:ivanakov@uns.ac.rs) (I. Kovacic).

is of interest for vibration isolation [1–3]. The second type arises in systems where the restoring force is purely nonlinear in nature. Practical examples of these systems are grounded in different fields of physics and engineering [4,5]. Some of them are micro-electro-mechanical systems: for instance, in an electrostatically operated micro mirror, the restoring force is proportional to the square of the deflection [6]; then, in a micro-actuator, the force–displacement relationship can have an exponent that ranges from 2 to 7 [7]. Further, suspension of the vehicle can be modelled in this way with the power being equal approximately to  $\frac{3}{2}$  [8,9]. Also, the interaction between the beads in the study of impulse propagation in a chain of elastic beads is characterized by the fractional-order potential with the exponent between 2.5 and 3 [10].

The conservative oscillators modelled by Eq. (1) with  $F=0$  have been the subject of the extensive research. Rosenberg [11] presented their solution for motion in the form of newly created special Ateb functions. However, for the sake of convenience, many later studies have been devoted to describing the motion by using the trigonometric functions [12–15] or elliptic functions, which have been used for quadratic and cubic oscillators only [16–20]. The oscillators with a single-term nonlinear restoring force are named ‘truly nonlinear oscillator’ by Mickens [21], whose work initiated series of papers in which these oscillators have been studied by different methods, such as the harmonic balance method, parameter expansions, iteration methods, variation methods, etc. (see, for example, [14–21] and the papers cited therein).

Among the papers concerned with the non-conservative oscillators modelled by Eq. (1), two main groups of studies can be distinguished. The first group of papers include those concerned with the oscillators with a fractional-order restoring force with the motion described by trigonometric functions. In [13], the van der Pol equation with  $\alpha = \frac{1}{3}$  was studied by using phase-space techniques and the Lienard–Levinson–Smith theorem. Waluya and van Horsen [22] used the perturbation method based on integrating factors to derive approximate first integrals for the van der Pol oscillator in which  $\alpha = (2m+1)/(2n+1)$ , and  $m, n \in N$ . In [23], analytical approximations to the period of a generalized van der Pol equation were obtained by using various asymptotic methods. In [14], the Krylov–Bogoliubov method was extended to find the first approximation of motion the frequency of which was calculated from the exact period of the corresponding conservative oscillator. According to the author, the method gives good approximations for  $1 \leq \alpha \leq 3$ . The second group of papers comprises studies of the oscillators with a polynomial (integer-power) restoring force with the motion described by elliptic functions. Quadratic oscillator have been investigated by applying the elliptic perturbation method [24], the elliptic multiple scales method [25] and the elliptic Lindstedt–Poincaré method [26]. Following this work, Chen et al. [27] have recently proposed a perturbation method for determining the homoclinic solution of non-conservative quadratic oscillators with a generative solution that has the form of a hyperbolic function. Cubic oscillators have been studied by using the elliptic multiple scales method [25], the elliptic harmonic balance method [28], the elliptic Krylov–Bogoliubov method [28–30] and the elliptic Lindstedt–Poincaré method [31].

Although the elliptic functions are sometimes considered to be more difficult to work with than trigonometric functions, this work can be considerably simplified, accelerated and made to be more efficient if computer algebra and symbolic software are used [17,18]. Motivated by these possibilities as well with the fact that an elliptic function includes higher harmonics in itself, which can be of paramount importance in nonlinear problems, we seek for the solution of motion of the oscillator modelled by Eq. (1) by assuming it in the form

$$x(t) = A \operatorname{cn}[\psi, m(\alpha)], \quad (3)$$

where  $A$  is an amplitude of motion, while  $\psi$ , which depends on the frequency of the Jacobi elliptic function, and the parameter  $m$  is unknown. It is proposed here to determine them from the energy conservation law and Hamilton’s variational principle, respectively, as the functions of the arbitrary power  $\alpha$ . The solution given by Eq. (3) is then used as a generative one for the extension of the Krylov–Bogoliubov method to find the motion of non-conservative oscillators. In comparison to the existing techniques, the methods proposed in this paper for both conservative and non-conservative cases do not have any limitations regarding the value of the power of the nonlinear restoring force, and, thus, cover wider range of theoretical and practical problems, which are also accompanied with the excellent accuracy of the solutions obtained regardless of the value of  $\alpha$ .

## 2. Conservative oscillator: generative solution

In this section, the conservative oscillators modelled by Eq. (1) with  $F=0$  are considered. Introducing non-dimensional (ND) displacement  $\xi$  and time  $\tau$

$$\xi = \frac{x}{X_0}, \quad \tau = \frac{t}{\sqrt{\frac{M}{C} X_0^{(1-\alpha)/2}}}. \quad (4)$$

Eqs. (1) and (2) become

$$\frac{d^2 \xi}{d\tau^2} + \operatorname{sgn}(\xi) |\xi|^\alpha = 0, \quad \xi(0) = 1, \quad \frac{d\xi}{d\tau}(0) = 0. \quad (5)$$

The corresponding energy integral of this system is

$$\frac{1}{2} \left( \frac{d\xi}{d\tau} \right)^2 + \frac{|\xi|^{\alpha+1}}{\alpha+1} = \frac{1}{\alpha+1}, \tag{6}$$

which yields the following expression for the period of oscillations [14,32]

$$T_{\text{ex}}^{\text{ND}} = 4 \int_0^1 \frac{d\xi}{\left| \frac{d\xi}{d\tau} \right|} = 4 \sqrt{\frac{\alpha+1}{2}} \int_0^1 \frac{d\xi}{\sqrt{1-|\xi|^{\alpha+1}}}. \tag{7}$$

The exact period can be expressed by means of the Euler Gamma function  $\Gamma$  and the power  $\alpha$  as follows [14,32]:

$$T_{\text{ex}}^{\text{ND}} = 4 \sqrt{\frac{\alpha+1}{2}} \frac{\sqrt{\pi} \Gamma \left[ 1 + \frac{1}{1+\alpha} \right]}{\Gamma \left[ \frac{1}{2} + \frac{1}{1+\alpha} \right]}. \tag{8}$$

Going back to dimensional variables and using Eq. (4), the period–amplitude relationship for the oscillators defined by Eq. (1) is

$$T_{\text{ex}}(A) = \sqrt{\frac{M}{C}} T_{\text{ex}}^{\text{ND}} A^{(1-\alpha)/2}, \tag{9}$$

where  $A$  corresponds to the initial displacement, i.e.  $A \equiv X_0$ .

A truly nonlinear character of the oscillators under consideration, i.e. the fact that the power  $\alpha$  can take any non-negative real value, is the motivation to assume the approximate solution for motion by using the cn Jacobi elliptic function in place of the usual trigonometric functions

$$\xi(\tau) = \text{cn}[\omega^{\text{ND}}(\alpha)\tau, m(\alpha)]. \tag{10}$$

The frequency  $\omega^{\text{ND}}$  of the elliptic function and the parameter of the elliptic function  $m$ , which can take the values from the interval  $-1 < m < 1$ , are unknown functions of the power  $\alpha$  and need to be specified.

Since it is known that the period of the cn Jacobi elliptic function is  $4K(m)$ , where  $K(m)$  is the complete elliptic integral of the first kind [33], the frequency  $\omega^{\text{ND}}(\alpha)$  can be related to this period by

$$\omega^{\text{ND}}(\alpha) = \frac{4K(m(\alpha))}{T_{\text{ex}}^{\text{ND}}(\alpha)}. \tag{11}$$

The parameter  $m$  can be determined by finding the extremum of Hamilton’s action integral [34]. The action integral is

$$I = \int_0^{K(m)/\omega^{\text{ND}}} L d\tau, \tag{12}$$

with  $L$  being the Lagrangian, which is defined as the kinetic energy of the system minus its potential energy

$$L = \frac{1}{2} \left( \frac{d\xi}{d\tau} \right)^2 - \frac{|\xi|^{\alpha+1}}{\alpha+1} = \frac{1}{2} (\omega^{\text{ND}})^2 \text{sn}^2[\omega^{\text{ND}}\tau, m] \text{dn}^2[\omega^{\text{ND}}\tau, m] - \frac{|\text{cn}[\omega^{\text{ND}}\tau, m]|^{\alpha+1}}{\alpha+1}. \tag{13}$$

The upper boundary in Eq. (12) corresponds to one fourth of the exact period in Eq. (8). Along this interval, the solution described by Eq. (10) is always positive and the absolute value in the integrand can be omitted.

Substituting Eq. (13) into Eq. (12) and using Eq. (11), the action integral becomes

$$I(\alpha, m) = \frac{K(m)[(2m-1)E(m)+K(m)-mK(m)]\Gamma\left(\frac{\alpha+3}{2(\alpha+1)}\right)}{3\sqrt{2\pi m}\sqrt{\alpha+1}\Gamma\left(\frac{\alpha+2}{\alpha+1}\right)} - \frac{\pi\Gamma\left(\frac{\alpha+2}{2}\right)\Gamma\left(\frac{\alpha+2}{\alpha+1}\right)\Phi_1}{2\sqrt{2}\sqrt{1+\alpha}K(m)\Gamma\left(\frac{\alpha+3}{2(\alpha+1)}\right)\Gamma\left(\frac{\alpha+3}{2}\right)}, \tag{14}$$

where  $E(m)$  denotes the complete elliptic integral of the second kind [33], and

$$\Phi_1 = {}_2F_1\left(\frac{1}{2}, \frac{1}{2}, \frac{3+\alpha}{2}, m\right), \tag{15}$$

stands for the Gauss hypergeometric function [33].

Now, in the sense of the Ritz method [34], the action integral in Eq. (14) should be stationary. Its variation is

$$\delta I = \frac{\partial I(\alpha, m)}{\partial m} \delta m \equiv 0, \tag{16}$$

which implies

$$\frac{\partial I}{\partial m} \equiv h(\alpha, m(\alpha)) = \frac{2^{-(5+9\alpha)/2(1+\alpha)}}{a_1} \left[ -4a_2(1+\alpha)K^2(m)\Gamma\left(\frac{1}{2} + \frac{1}{1+\alpha}\right)^2 - a_3a_4 \right] = 0, \quad (17)$$

where

$$a_1 = 3\pi(m-1)m^2\sqrt{1+\alpha}K^2(m)\Gamma\left(\frac{2}{1+\alpha}\right), \quad (18)$$

$$a_2 = (2m-1)E^2(m) - 4(m-1)E(m)K(m) + 3(m-1)K^2(m), \quad (19)$$

$$a_3 = \frac{3\pi^2m}{\Gamma\left(\frac{3+\alpha}{2}\right)} 2^{-\alpha}\Gamma^2\left(\frac{1}{1+\alpha}\right)\Gamma(1+\alpha), \quad (20)$$

$$a_4 = \frac{1}{\Gamma\left(\frac{\alpha+3}{2}\right)} [E(m)\Phi_1 + (m-1)K(m)\Phi_2], \quad (21)$$

with  $\Phi_2$  representing the following hypergeometric function:

$$\Phi_2 = {}_2F_1\left(\frac{3}{2}, \frac{1}{2}, \frac{3+\alpha}{2}, m\right). \quad (22)$$

It should be noted that the expression for  $a_1$  imposes the condition  $m \neq 0$ , which corresponds to the linear restoring force. In this case, the solution in Eq. (10) simplifies to the trigonometric Cosine function, and thus, the condition defined by Eq. (16) is not needed. However, it can be shown that when  $\alpha \rightarrow 1$ , Eq. (17) yields  $m \rightarrow 0$ . For other cases, the function  $h(\alpha, m(\alpha))$  given by Eq. (17) defines implicitly how the parameter  $m$  depends on the power  $\alpha$ . This dependence is presented graphically in Fig. 1. In the case of a pure cubic oscillator, i.e. when  $\alpha = 3$ , one has  $m = 0.5$ , which is the well known result [28].

The parameter  $m$  can be obtained by solving Eq. (17) numerically for a given value of the power  $\alpha$ , and then  $\omega^{\text{ND}}$  can be calculated from Eq. (11). Their values corresponding to certain values of the power  $\alpha$  are given in Table 1.

It is seen from Fig. 1 and Table 1 that for  $\alpha$  higher than unity (over-linear case), the parameter  $m$  is positive. When  $\alpha$  is less than unity (under-linear case), the parameter  $m$  is negative. As the parameter  $m$  represents the square of the modulus  $k$ , i.e.  $m = k^2$  [35], it follows that  $k$  is imaginary in the under-linear case. It should be noted that the Jacobi cn functions with an imaginary modulus can be converted into the one with the modulus whose value is in the range (0, 1) by using [36]

$$\text{cn}\left[k'u, \frac{ik'}{k'}\right] = \frac{\text{cn}[u, k]}{\text{dn}[u, k]}, \quad (23)$$

where  $k' = \sqrt{1-k^2}$ . This transformation is important for the reader who would use symbolic software without inbuilt Jacobi functions with the imaginary modulus. However, contemporary computer algebra software recognizes Jacobi functions with the imaginary modulus and automatically performs this conversion.

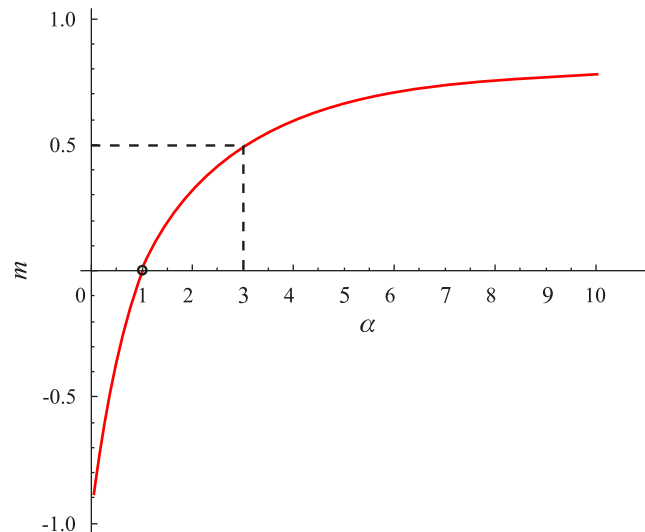
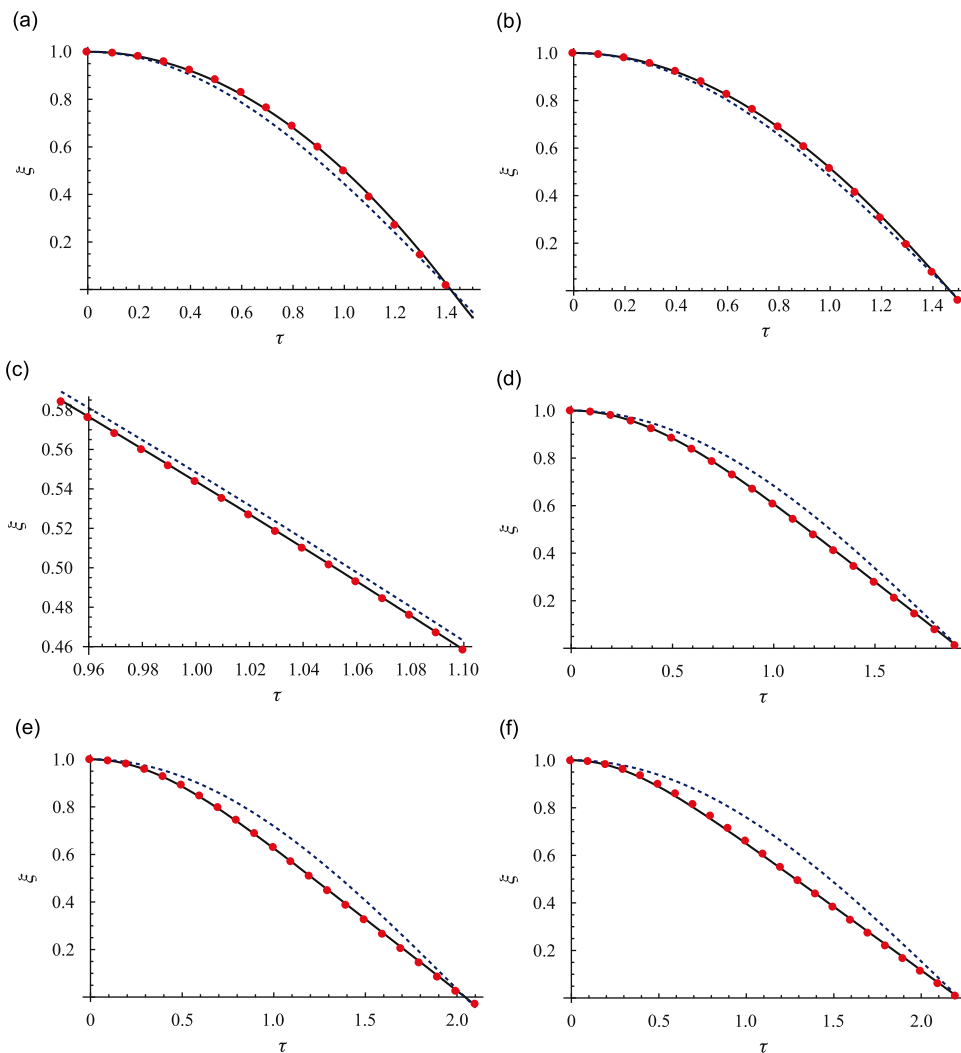


Fig. 1. Parameter  $m$  defined by Eq. (17) versus the power  $\alpha$  and a circle indicates that  $m=0$  when  $\alpha=1$  and a dashed line that  $m=\frac{1}{2}$  when  $\alpha=3$ .

**Table 1**

Values of the parameter  $m$ , frequency  $\omega^{ND}$  and correction factor  $d$  for some values of the power  $\alpha$ .

$\alpha$	$m$ Eq. (17)	$\omega^{ND}$ Eq. (11)	$d$ Eq. (43)
0	-0.878083	0.942948	0.756691
1/10	-0.737477	0.952046	0.717454
1/3	-0.47129	0.969686	0.6415
1/2	-0.321203	0.979709	0.597547
1.1	0.0478074	1.00263	0.484987
3/2	0.202556	1.00947	0.435285
2	0.337834	1.01129	0.390168
5/2	0.432067	1.00761	0.357573
3	0.5	1	1/3
7/2	0.550448	0.989667	0.314851
4	0.588907	0.97752	0.300438
9/2	0.618919	0.964235	0.28897
5	0.642829	0.950301	0.279679
6	0.678236	0.921786	0.265637



**Fig. 2.** Comparisons of the approximate solution given by (10), (11) and (17) (circles) with the numerical solution of the equation of motion (5) (solid line) and the first approximation from [14] (dotted line) for different values of the power  $\alpha$ : (a)  $\alpha = 0$ ; (b)  $\alpha = \frac{1}{3}$ ; (c)  $\alpha = 1.1$ ; (d)  $\alpha = 3.5$ ; (e)  $\alpha = 4.5$ ; and (f)  $\alpha = 6$ .

In order to check the accuracy of the solutions obtained, the approximate solution defined by Eq. (10) is plotted in Fig. 2 for several values of the power  $\alpha$  and it is depicted by circles. In addition, in Figs. 2a–f numerical solutions obtained by direct integration of Eq. (5) are also shown as solid lines, as well as the approximate solution that uses the Cosine function with the exact period [14], which is plotted as a dotted line. These comparisons illustrate excellent accuracy of the solution obtained, even for very small values of the power  $\alpha$  or very high ones. However, this is when the first approximation in the form of the Cosine solution [14] fails to predict the response satisfactory, since the higher harmonics are not included into time histories, while the elliptic solution captures them well. It should also be emphasized that the solution obtained for the case  $\alpha = 0$  (Fig. 2a), which corresponds to the so-called antisymmetric oscillator, is in excellent agreement with the numerical one. Unlike its exact solution expressed in the form of a non-periodic square polynomial [21], the solution found herein has the form of a periodic function, which is thus valid for an arbitrary time interval. In order to present the match and the difference between the results clearly, only the solutions corresponding to one fourth of the period are shown, with the exception of the case  $\alpha = 1.1$  (Fig. 2c), when even a smaller time interval is plotted for clarity.

The approximate solution constructed for the conservative case can be used now as a generating solution for non-conservative oscillators.

### 3. Non-conservative oscillator: Krylov–Bogoliubov method

By introducing the non-dimensional variables given in Eqs. (4), (1) and (2) can be written down as

$$\frac{d^2\xi}{d\tau^2} + \varepsilon f\left(\xi, \frac{d\xi}{d\tau}\right) + \text{sgn}(\xi)|\xi|^\alpha = 0, \quad \xi(0) \equiv \bar{A} = 1, \quad \frac{d\xi}{d\tau}(0) = 0, \quad (24)$$

where  $\varepsilon f(\xi, d\xi/d\tau)$  is the non-dimensional form of the force  $F(x, \dot{x})$ . It is assumed here that  $\varepsilon \ll 1$ , i.e. that the term  $\varepsilon f(\xi, d\xi/d\tau)$  represents a small perturbation of the conservative oscillator governed by Eq. (5).

In order to find the approximate solution of the non-conservative oscillators modelled by Eq. (24), the so-called generative solution is assumed in the form defined by Eq. (10), i.e. as  $\xi = \bar{A} \text{cn}[\omega^{\text{ND}}(\alpha)\tau, m(\alpha)]$ , and with the velocity given by

$$\frac{d\xi}{d\tau} = -\omega^{\text{ND}} \bar{A} \text{sn}[\omega^{\text{ND}}\tau, m] \text{dn}[\omega^{\text{ND}}\tau, m], \quad (25)$$

which satisfy Eq. (24) exactly to zero order ( $\varepsilon = 0$ ), i.e.

$$-(\omega^{\text{ND}})^2 \bar{A}^2 \text{cn}[\omega^{\text{ND}}\tau, m] \text{dn}^2[\omega^{\text{ND}}\tau, m] + (\omega^{\text{ND}})^2 \bar{A} m \text{sn}^2[\omega^{\text{ND}}\tau, m] \text{cn}[\omega^{\text{ND}}\tau, m] + \bar{A}^\alpha \text{sgn}(\text{cn}[\omega^{\text{ND}}\tau, m]) |\text{cn}[\omega^{\text{ND}}\tau, m]|^\alpha = 0. \quad (26)$$

It is assumed now that the non-dimensional amplitude (equal to unity for the conservative case) and phase (equal to zero for the conservative case) are not constant anymore, but change very slowly with time, so that the trial solution has the form

$$\xi(\tau) = a(\tau) \text{cn}[\psi(\tau), m], \quad (27)$$

with the unknown complete phase  $\psi(\tau)$  being defined by

$$\psi(\tau) = \int \omega(a) ds + \varphi(\tau), \quad (28)$$

where the phase  $\varphi(\tau)$  also needs to be determined.

Further, the frequency-amplitude relationship  $\omega(a)$  can be found from the analogy with this relationship corresponding to the conservative case, which is the idea proposed by Cveticanin [14]. Eq. (9) implies that the period of conservative oscillators is proportional to  $A^{(1-\alpha)/2}$ , where  $A$  is the initial amplitude. Thus, the frequency is proportional to  $A^{(\alpha-1)/2}$ . Bearing in mind that the non-conservative oscillators under consideration can be treated as small perturbation of the conservative ones, one can assume that their frequency changes with the amplitude in the same way

$$\omega(a) = \omega^{\text{ND}} a^{(\alpha-1)/2}, \quad (29)$$

but the amplitude  $a$  slowly varies with time.

The next assumption of the Krylov–Bogoliubov method is that the time derivative of the solution from Eq. (27) has the same form as the velocity given by Eq. (25), i.e.

$$\frac{d\xi}{d\tau} = -\omega a \text{sn} \text{dn}, \quad (30)$$

as a result of which the following constraint is derived

$$\frac{da}{d\tau} \text{cn} - a \frac{d\varphi}{d\tau} \text{sn} \text{dn} = 0, \quad (31)$$

where

$$\operatorname{sn} \equiv \operatorname{sn}[\psi(\tau), m], \quad \operatorname{cn} \equiv \operatorname{cn}[\psi(\tau), m], \quad \operatorname{dn} \equiv \operatorname{dn}[\psi(\tau), m]. \tag{32}$$

In addition, the trial solution should satisfy the same condition as the generating one given by Eq. (26)

$$-\omega^2 a \operatorname{cn} \operatorname{dn}^2 + \omega^2 a m \operatorname{sn}^2 \operatorname{cn} + a^\alpha \operatorname{sgn}(\operatorname{cn}) |\operatorname{cn}|^\alpha = 0. \tag{33}$$

Then, differentiating Eq. (30) once and substituting it into the equation of motion written in Eq. (24), gives

$$-\frac{da}{d\tau} \omega \operatorname{sn} \operatorname{dn} - a \frac{d\omega}{d\tau} \operatorname{sn} \operatorname{dn} - a\omega \frac{d\varphi}{d\tau} \operatorname{cn}(1-2m \operatorname{sn}^2) - \omega^2 a \operatorname{cn} \operatorname{dn}^2 + \omega^2 a m \operatorname{sn}^2 \operatorname{cn} + a^\alpha \operatorname{sgn}(\operatorname{cn}) |\operatorname{cn}|^\alpha = -\varepsilon f(a \operatorname{cn}, -a\omega \operatorname{sn} \operatorname{dn}). \tag{34}$$

Taking into account Eqs. (33) and (34) becomes

$$-\frac{da}{d\tau} \omega \operatorname{sn} \operatorname{dn} - a \frac{d\omega}{d\tau} \operatorname{sn} \operatorname{dn} - a\omega \frac{d\varphi}{d\tau} \operatorname{cn}(1-2m \operatorname{sn}^2) = -\varepsilon f(a \operatorname{cn}, -a\omega \operatorname{sn} \operatorname{dn}). \tag{35}$$

Combining Eqs. (31) and (35), one obtains

$$\frac{da}{d\tau} \omega [\operatorname{sn}^2 \operatorname{dn}^2 + \operatorname{cn}^2(1-2m \operatorname{sn}^2)] + a \frac{d\omega}{d\tau} \operatorname{sn}^2 \operatorname{dn}^2 = \varepsilon f(a \operatorname{cn}, -a\omega \operatorname{sn} \operatorname{dn}) \operatorname{sn} \operatorname{dn}, \tag{36}$$

$$\frac{d\varphi}{d\tau} a\omega [\operatorname{sn}^2 \operatorname{dn}^2 + \operatorname{cn}^2(1-2m \operatorname{sn}^2)] + a \frac{d\omega}{d\tau} \operatorname{sn} \operatorname{cn} \operatorname{dn} = \varepsilon f(a \operatorname{cn}, -a\omega \operatorname{sn} \operatorname{dn}) \operatorname{cn}. \tag{37}$$

The time derivative  $d\omega/d\tau$  is obtained from Eq. (29):

$$\frac{d\omega}{d\tau} = \omega(a) \frac{\alpha-1}{2a} \frac{da}{d\tau}. \tag{38}$$

Introducing Eq. (38) into Eqs. (36) and (37), gives

$$\frac{da}{d\tau} \omega(a) \left[ \operatorname{sn}^2 \operatorname{dn}^2 \frac{\alpha+1}{2} + \operatorname{cn}^2(1-2m \operatorname{sn}^2) \right] = \varepsilon f(a \operatorname{cn}, -a\omega \operatorname{sn} \operatorname{dn}) \operatorname{sn} \operatorname{dn}, \tag{39}$$

$$\frac{d\varphi}{d\tau} a\omega [\operatorname{sn}^2 \operatorname{dn}^2 + \operatorname{cn}^2(1-2m \operatorname{sn}^2)] + \omega(a) \frac{\alpha-1}{2} \frac{da}{d\tau} \operatorname{sn} \operatorname{cn} \operatorname{dn} = \varepsilon f(a \operatorname{cn}, -a\omega \operatorname{sn} \operatorname{dn}) \operatorname{cn}. \tag{40}$$

One can proceed by observing that Eqs. (39) and (40) are periodic in  $\psi$  with period  $4K(m)$ . Therefore, averaging over this period, one derives

$$\frac{da}{d\tau} = \frac{1}{d} \frac{\varepsilon}{\omega(a)} \frac{2}{\alpha+3} \frac{1}{4K(m)} \int_0^{4K(m)} f(a \operatorname{cn}, -a\omega \operatorname{sn} \operatorname{dn}) \operatorname{sn} \operatorname{dn} \operatorname{d}\psi, \tag{41}$$

$$\frac{d\varphi}{d\tau} = \frac{1}{d} \frac{\varepsilon}{2a\omega(a)} \frac{1}{4K(m)} \int_0^{4K(m)} f(a \operatorname{cn}, -a\omega \operatorname{sn} \operatorname{dn}) \operatorname{cn} \operatorname{d}\psi, \tag{42}$$

where  $d$  is named a ‘correction factor’ after its constant value and is given by

$$d = \frac{(2m-1)E(\theta, m) - 4(m-1)K(m)}{12mK(m)}, \tag{43}$$

with  $E(\theta, m)$  being equal to the incomplete elliptic integral of the second kind and  $\theta = \operatorname{am}[4K(m), m]$  being the elliptic amplitude function.

By solving Eqs. (41) and (42), with the parameter  $m$  calculated from Eq. (17), the solutions for the amplitude and phase of the oscillator in Eq. (24) can be obtained. On the basis of Eqs. (24) and (27), their initial values are

$$a(0) = 1, \quad \psi(0) = 0. \tag{44}$$

Finally, taking into account the relationships from Eq. (4), the solution for motion of Eq. (1) can be found.

Some remarks can be made here regarding the forms of Eqs. (41) and (42) for some special values of the power  $\alpha$ . In all of them, the correction factor appears, which represents a constant defined by Eq. (43) for the parameter  $m$  specified by Eq. (17). Thus, this correction factor depends on the power  $\alpha$ , as illustrated in Fig. 3. Its values are also listed in Table 1 for some values of the power  $\alpha$ . When the oscillator is linear, i.e.  $\alpha = 1$ , the parameter  $m$  tends to zero, the elliptic function turns into a Cosine function and the correction factor  $d$  defined by Eq. (43) tends to  $\frac{1}{2}$ . Then, the well-known equations for the derivatives of the amplitude and phase of the classical Krylov–Bogoliubov method are derived [37]:

$$\frac{da}{d\tau} = \frac{\varepsilon}{2\pi} \int_0^{2\pi} f(a \cos \psi, -a\omega \sin \psi) \sin \psi \operatorname{d}\psi, \tag{45}$$

$$\frac{d\varphi}{d\tau} = \frac{\varepsilon}{2\pi a} \int_0^{2\pi} f(a \cos \psi, -a\omega \sin \psi) \cos \psi \operatorname{d}\psi. \tag{46}$$

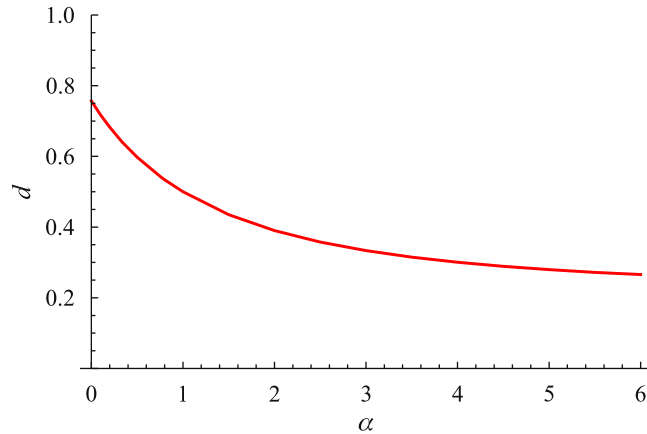


Fig. 3. Correction factor  $d$  defined by Eqs. (43) and (17) versus the power  $\alpha$ .

In the case of pure-cubic oscillators, i.e. when  $\alpha = 3$ , one calculates  $d = \frac{1}{3}$ , which gives the following equation for the derivatives of the amplitude and phase:

$$\frac{da}{d\tau} = \frac{\varepsilon}{\omega(a)} \frac{1}{4K(1/2)} \int_0^{4K(1/2)} f(a \operatorname{cn}, -a\omega \operatorname{sn} \operatorname{dn}) \operatorname{sn} \operatorname{dn} d\psi, \quad (47)$$

$$\frac{d\varphi}{d\tau} = \frac{3}{2} \frac{\varepsilon}{a\omega(a)} \frac{1}{4K(1/2)} \int_0^{4K(1/2)} f(a \operatorname{cn}, -a\omega \operatorname{sn} \operatorname{dn}) \operatorname{cn} d\psi. \quad (48)$$

Eq. (47) coincides with the form derived in [29]. The expression for the phase given by Eq. (48) is slightly different from the one derived in [29,30], which will be discussed later in Section 4.3.

The above special cases and their examination allows a fuller understanding of the generality of the derived equations for the amplitude and phase. The next section gives several examples that illustrate their use and advantages.

## 4. Examples

### 4.1. Polynomial damping force

When the damping force in Eq. (1) has the form

$$F(x, \dot{x}) = b \operatorname{sgn}(\dot{x}) |\dot{x}|^\beta, \quad (49)$$

the non-dimensional coefficient  $\varepsilon$  is

$$\varepsilon = \frac{bC^{(\beta-2)/2}}{M^{\beta/2}} X_0^{\beta(1+\alpha)/2-\alpha}. \quad (50)$$

Three cases will be considered here  $\beta = 1, 2$  and  $0$ , which correspond to linear viscous damping, quadratic damping and dry friction, respectively. They all belong to the so-called positive damping [38], as they cause the amplitude of the unforced motion to decrease. Of interest here is to obtain approximations for damped transient solutions of the oscillators with a non-negative real-power restoring force. It will be shown how the method proposed above helps in their physical understanding, which includes the change of their amplitudes and phases.

#### 4.1.1. Linear damping

For the case of linear damping, one has  $\beta = 1$ ,  $\varepsilon = (b/\sqrt{CM})X_0^{(1-\alpha)/2}$ , so that Eqs. (41), (42) and (28) yield

$$a(\tau) = \exp\left(-\frac{2\varepsilon}{\alpha+3}\tau\right), \quad (51)$$

$$\varphi = 0, \quad (52)$$

$$\psi(\tau) = \frac{\omega^{\text{ND}}(\alpha+3)}{(\alpha-1)\varepsilon} \left(1 - \exp\left(-\frac{\alpha-1}{\alpha+3}\varepsilon\tau\right)\right). \quad (53)$$

Eq. (51) implies that the amplitude changes exponentially with time. When  $\varepsilon$  is fixed, the higher the values of the power  $\alpha$ , the higher the relative maxima of the amplitude.



If the equation of motion and the initial conditions are

$$\ddot{x} + \dot{x} + \pi \operatorname{sgn}(x)|x|^{3.5} = 0, \quad x(0) = 5, \quad \dot{x}(0) = 0, \tag{54}$$

the approximation for motion is

$$x(t) = 5 \exp(-0.307692t) \operatorname{cn}[34.0996(1 - (\exp(-0.307692t))^{1.25}), 0.550448]. \tag{55}$$

This approximate solution is plotted in Fig. 4 in circles together with the numerical solution, which is shown as a solid line. Despite the fact that the decay of the oscillation is very rapid and that the nonlinearity in Eq. (54) is strong, there is very good agreement between the solutions. In order to quantify the difference between the analytical and numerical solutions, the percentage error is calculated between the relative extremum calculated numerically and the analytical result for the displacement corresponding to the time when this relative extremum is achieved. This error is then averaged for all the relative extrema shown in the figure where the solutions are plotted (this averaged percentage error will subsequently be referred to as  $\bar{\Delta}$ ). Thus, the averaged percentage error calculated for 9 extrema shown in Fig. 4 is  $\bar{\Delta} = 0.023\%$ .

The approximate solution for the velocity  $v(t)$ , found by differentiating Eq. (55) is determined and plotted in circles in Fig. 5 together with the numerical solution (solid line). The agreement between the solutions is very good.

#### 4.1.2. Quadratic damping

When  $\beta = 2$ , the parameter  $\varepsilon$  is  $\varepsilon = (b/M)X_0$ . By using Eq. (41), the solution for the amplitude is derived

$$a(\tau) = (1 + \varepsilon \delta \tau)^{-2/(\alpha+1)}, \tag{56}$$

where

$$\delta = \frac{2\omega^{\text{ND}}(5-4m)(\alpha+1)}{15d(\alpha+3)K(m)}. \tag{57}$$

According to Eq. (56), the amplitude changes algebraically with time. If  $\varepsilon$  is fixed, the higher the values of the power  $\alpha$ , the higher relative maxima of the amplitude.

The complete phase is obtained from Eqs. (42) and (28)

$$\psi(\tau) = \frac{\omega^{\text{ND}}(\alpha+1)}{2\varepsilon\delta} (1 - (1 + \varepsilon \delta \tau)^{2/(\alpha+1)}).$$

The solution for motion of the oscillator

$$2\ddot{x} + \operatorname{sgn}(\dot{x})(\dot{x})^2 + \operatorname{sgn}(x)|x|^{2\pi} = 0, \quad x(0) = 1, \quad \dot{x}(0) = 0. \tag{58}$$

is

$$x(t) = (1 + 0.141298t)^{-2/(1+2\pi)} \operatorname{cn}[16.651879(1 - (1 + 0.141298t)^{-2/(1+2\pi)}), 0.686102]. \tag{59}$$

In Fig. 6 this approximate analytical and the numerical solution are plotted in circles and as a solid line, respectively. The amplitude curve defined by Eq. (56) is also presented. A very good match between the solutions is evident. The averaged percentage error calculated for 4 extrema shown in Fig. 6 is  $\bar{\Delta} = 0.68\%$ .

In order to demonstrate that the procedure is also convenient and reliable for small values of  $\alpha$ , the following oscillator is considered:

$$4\ddot{x} + 0.5 \operatorname{sgn}(\dot{x})\dot{x}^2 + \operatorname{sgn}(x)|x|^{1/3} = 0, \quad x(0) = 1, \quad \dot{x}(0) = 0, \tag{60}$$

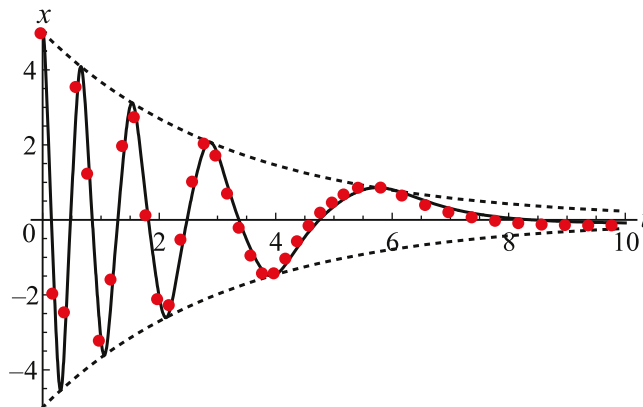


Fig. 4. Approximate solution for motion Eq. (55) (circles) and the numerical solution (solid line) of the oscillator modelled by Eq. (54) and dotted lines depicts the approximate solution for the amplitude (51).

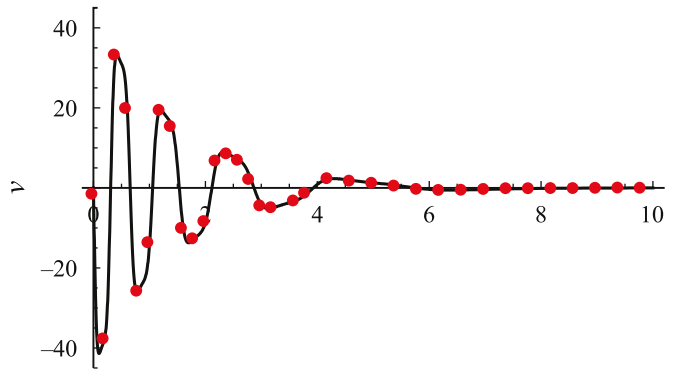


Fig. 5. Approximate solution for velocity (circles) and the numerical solution (solid line) of the oscillator modelled by Eq. (54).

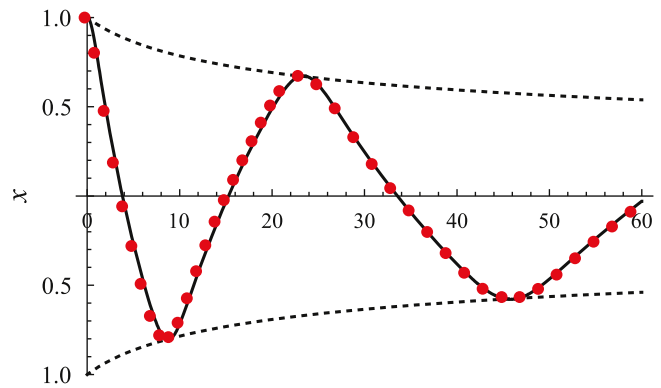


Fig. 6. Approximate solution for motion Eq. (59) (circles) and the numerical solution (solid line) of the oscillator modelled by Eq. (58) and dotted lines depicts the approximate solution for the amplitude Eq. (56).

the solution of which is

$$x(t) = \frac{\text{cn}[13.2577 - 0.0668855\sqrt{1 + 0.0243805t}(198.214 + 4.83257t), -0.47129]}{(1 + 0.0243805t)^{3/2}} \tag{61}$$

This solution is shown in Fig. 7 and a good match with the numerical solution is evident. For the extrema shown in this figure, the average percentage error is  $\bar{\Delta} = 0.25\%$ .

#### 4.1.3. Dry friction

For the case of dry friction, the force  $F$  in Eq. (1) is given by  $F = b \text{sgn}(\dot{x})$ , where the coefficient  $b$  is proportional to the normal force. The dead zone is

$$-x_d < x < x_d, \quad x_d = \left(\frac{b}{C}\right)^{1/\alpha} \tag{62}$$

For this system, the parameter  $\beta = 0$  and hence,  $\varepsilon = b/(CX_0^\alpha)$ , which yields

$$-\varepsilon^{1/\alpha} < \xi < \varepsilon^{1/\alpha} \tag{63}$$

By using Eq. (41), the solution for the amplitude is obtained

$$a(\tau) = (1 - \varepsilon q \tau)^{2/(\alpha+1)}, \tag{64}$$

where

$$q = \frac{(\alpha + 1)}{\omega^{\text{ND}} d(\alpha + 3) K(m)}. \tag{65}$$

Comparing the amplitude law for the case of dry friction Eq. (64) with the one for quadratic damping Eq. (56), one can see that their exponents are, respectively,  $2/(1 + \alpha)$  and  $-2/(1 + \alpha)$ , i.e. they are of the opposite sign. A base in these amplitude laws is a linear function of time, which in the case of dry friction has a negative slope, and in the case of quadratic damping the positive one.

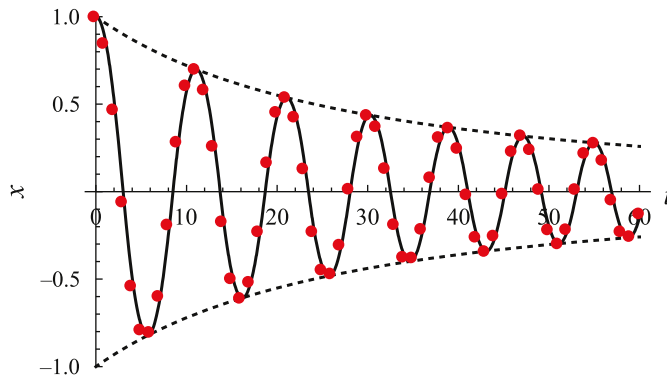


**Fig. 7.** Approximate solution for motion Eq. (61) (circles) and the numerical solution (solid line) of the oscillator modelled by Eq. (60) and dotted lines depicts the approximate solution for the amplitude.

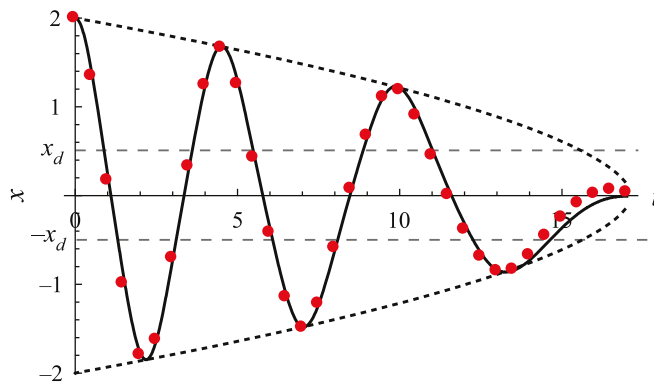


**Fig. 8.** Approximate solution for motion Eq. (70) (circles) and the numerical solution (solid line) of the oscillator modelled by Eq. (69); dotted lines depicts the approximate solution for the amplitude in Eq. (70) and gray dashed lines depict the dead zone defined by Eq. (62).

The complete phase derived from Eqs. (42) and (28) is

$$\psi(\tau) = \frac{\omega^{ND}(\alpha + 1)}{2\alpha\epsilon q} (1 - (1 - \epsilon p \tau)^{2\alpha/(1+\alpha)}). \tag{66}$$

It should be noted that Eq. (64) implies that there is the moment of time  $\tau^*$  for which  $a(\tau^*) = 0$ . It is defined by

$$\tau^* = \frac{1}{\epsilon q}, \tag{67}$$

which is when the oscillations cease. As the power  $\alpha$  increases, the value of  $q$  defined by Eq. (65) increases, too, so that  $\tau^*$  decreases.

In the special case when  $\alpha = 3$ , one obtains the dimensional time

$$T_{\alpha=3}^* = \frac{X_0^2 \sqrt{MCK} (\frac{1}{2})^2 \Gamma(\frac{3}{4})}{2\sqrt{2\pi} b \Gamma(\frac{5}{4})}, \tag{68}$$

which coincides with the result given in [30] (p. 273, Table 1).

For the oscillator

$$\ddot{x} + 0.2 \operatorname{sgn}(\dot{x}) + \operatorname{sgn}(x)x^{2.5} = 0, \quad x(0) = 2, \dot{x}(0) = 0, \tag{69}$$

the approximate solution for motion is

$$x(t) = 2(1 - 0.0583t)^{0.571429} \operatorname{cn}[20.3359(1 - (1 - 0.0583t)^{1.42857}), 0.432066]. \tag{70}$$

This solution is presented in Fig. 8 together with the numerical solution (solid line). The match between them is good. For the extrema shown in this Fig. 8, the average percentage error is  $\bar{\Delta} = 0.05\%$ .

#### 4.2. Van der Pol damping

Here, the case of damping related to the van der Pol oscillator is considered. This nonlinear damping mechanism dissipates energy for large displacements and feeds energy for small displacements, as a result of which the system reaches a limit cycle. Of interest here is to obtain analytically the solution for transient motion as well as the amplitude of the limit cycle of the systems with a fractional-order restoring force.

The damping function in Eq. (1) is assumed as  $F(x, \dot{x}) = \gamma(r^2 x^2 - p^2)\dot{x}$ . In this case, it is convenient to introduce the non-dimensional displacement as  $\xi = rx/p$  and the non-dimensional time as  $\tau = t/(\sqrt{M/C}(p/r)^{(1-\alpha)/2})$ , so that the equation of motion and the initial conditions get the form

$$\frac{d^2 \xi}{d\tau^2} + \varepsilon(\xi^2 - 1)\frac{d\xi}{d\tau} + \text{sgn}(\xi)|\xi|^\alpha = 0, \quad \xi(0) = \frac{r}{p}X_0, \quad \frac{d\xi}{d\tau}(0) = 0, \quad (71)$$

where the well-known form of the van der Pol damping term can be recognized [38], and where

$$\varepsilon = \frac{1}{\sqrt{MC}}\gamma p^2 \left(\frac{p}{r}\right)^{(1-\alpha)/2}. \quad (72)$$

Using Eq. (41) gives

$$\frac{da}{d\tau} = \frac{2\varepsilon}{(\alpha+3)}a(1-Ba^2), \quad (73)$$

where

$$B = \frac{2[1+m(m-1)]E(\theta, m) - 4[2+m(m-3)]K(m)}{5m[(2m-1)E(\theta, m) - 4(m-1)K(m)]}. \quad (74)$$

It is interesting to note that when  $\alpha \rightarrow 1$ , one has  $m \rightarrow 0$  and  $B \rightarrow \frac{1}{4}$ . In this way, the well-known expression for the amplitude equation on the classical van der Pol oscillator with a linear restoring force is obtained [39,40]

$$\frac{da}{d\tau} = \frac{\varepsilon}{2}a\left(1 - \frac{1}{4}a^2\right). \quad (75)$$

After integrating Eq. (73), one finds

$$a(\tau) = \frac{1}{\sqrt{\exp(-D\tau)\left(\frac{1}{a_0^2} - B\right) + B}}, \quad (76)$$

where

$$D = \frac{4\varepsilon}{\alpha+3}. \quad (77)$$

The steady-state amplitude  $a^*$ , i.e. the amplitude of the limit cycle follows from Eq. (76) for  $\tau \rightarrow \infty$ :

$$a^* = B^{-1/2}. \quad (78)$$

The change of this amplitude with the parameter  $\alpha$  is plotted in Fig. 9 in circles. This solution is in excellent agreement with the numerical solution presented as a solid line. As  $\alpha$  increases, the amplitude of the limit cycle slowly decreases. For  $\alpha < 1$ ,

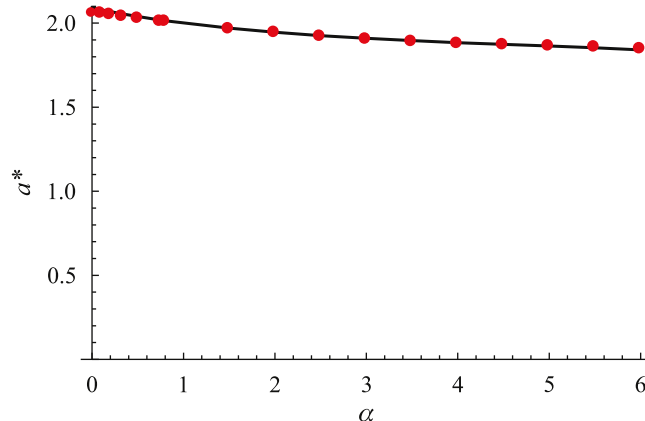


**Fig. 9.** Steady-state amplitude of the oscillator with van der Pol damping obtained approximately Eqs. (74) and (78) (circles) and the numerical solution (solid line).

one has  $a^* > 2$ , and for  $\alpha > 1$ , it is  $a^* < 2$ . It should be noted that this dependence is obtained in the first approximation. However, when one wants to determine it by using trigonometric functions, the second approximation is needed. This is because the first approximation of the solution in trigonometric functions does not show the influence of the power of the restoring force on the amplitude of the limit cycle [21], while the approximation obtained here does.

By using Eqs. (42) and (28), the complete phase is obtained

$$\psi(\tau) = \frac{4\omega^{ND}}{D(\alpha-1)} \left[ -\tilde{B}^{(1-\alpha)/4} \Phi_3 + \left( \frac{B + \tilde{B}\exp(-D\tau)}{1 + \frac{\tilde{B}}{B}\exp(D\tau)} \right)^{(1-\alpha)/4} \Phi_4 \right], \tag{79}$$

where

$$\tilde{B} = \frac{1}{a_0^2} - B, \tag{80}$$

with  $a_0 = rX_0/p$ ;  $\Phi_3$  and  $\Phi_4$  are the following hypergeometric functions

$$\Phi_3 = {}_2F_1\left(\frac{\alpha-1}{4}, \frac{\alpha-1}{4}, \frac{\alpha+3}{4}, -\frac{B}{\tilde{B}}\right), \tag{81}$$

$$\Phi_4 = {}_2F_1\left(\frac{\alpha-1}{4}, \frac{\alpha-1}{4}, \frac{\alpha+3}{4}, -\frac{B}{\tilde{B}}\exp(D\tau)\right). \tag{82}$$

Next, the following oscillator is considered:

$$\ddot{x} - 2(0.16 - 0.04x^2)\dot{x} + 3 \operatorname{sgn}(x)|x|^{5/2} = 0, \quad x(0) = 0.5, \quad \dot{x}(0) = 0 \tag{83}$$

and its numerically obtained motion is plotted in Fig. 10 together with the approximate solution defined by Eqs. (76) and (79). Figs. 10a shows the initial transient motion reaching the steady-state amplitude and the analytically obtained amplitude given by Eq. (76) being its envelope. In Fig. 10b both numerical and analytical time histories are shown in the steady state, confirming excellent agreement between the solutions. The amplitude of the steady-state solution calculated from Eq. (78) is  $a_{apr}^* = 3.85331$ , while the value found by integrating the equation of motion numerically is  $a_{num}^* = 3.85233$ .

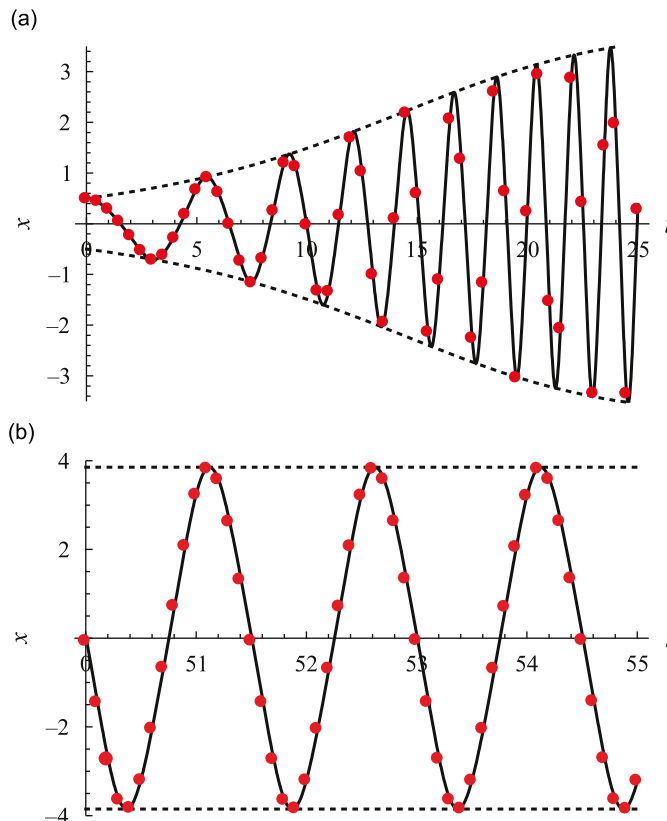


**Fig. 10.** Approximate solution for motion (circles) and the numerical solution (solid line) of the oscillator modelled by Eq. (83) and dotted lines depicts the approximate solution for the amplitude Eqs. (76) and (78): (a) transient solution and (b) steady-state solution.

The percentage error  $\Delta$  is

$$\Delta = \left| \frac{a_{apr}^* - a_{num}^*}{a_{num}^*} \right| \times 100 \approx 0.025\%, \quad (84)$$

which can be considered as negligible.

#### 4.3. Perturbative term is a linear function of the displacement

In this section, the force  $F$  in Eq. (1) is assumed in the form

$$F = cx, \quad (85)$$

where  $c$  is a constant that need not be small. After introducing the non-dimensional variables from Eq. (4), the parameter in front of the linear term is

$$\varepsilon = \frac{c}{C} X_0^{1-\alpha}. \quad (86)$$

Using Eqs. (41) and (42), leads to

$$a = 1, \quad (87)$$

$$\varphi(\tau) = \frac{\varepsilon[E(\theta, m) + 4(m-1)K(m)]}{8md\omega^{ND}K(m)} \tau, \quad (88)$$

where the fact that  $\varphi(0) = 0$  has been used.

The following oscillator is considered:

$$\ddot{x} + x^3 + 0.1x = 0, \quad x(0) = 1, \quad \dot{x}(0) = 0. \quad (89)$$

Its solution obtained by employing Eqs. (87), (88) and (4) is

$$x(t) = \text{cn}[1.0685419t, \frac{1}{2}]. \quad (90)$$

In [30], the authors examined the same equation on the basis of the first-order differential equation for the amplitude which corresponds to Eq. (47), and the equation for the phase

$$\frac{d\varphi^{yB}}{d\tau} = \frac{\varepsilon}{a\omega} \frac{1}{4K(1/2)} \int_0^{4K(1/2)} f(a \text{cn}, -a\omega \text{sn dn}) \text{cn} \, d\psi. \quad (91)$$

Their solution for motion is

$$x^{yB}(t) = \text{cn}[1.0456946t, \frac{1}{2}], \quad (92)$$

which is shown in Fig. 11 as a dashed line. The exact numerical solution is present also in this figure by solid lines, while the solution defined by Eq. (90), obtained by the method proposed in this paper, is plotted in circles. The difference between the approximate solutions given by Eqs. (90) and (92) stems from value of the correction factor  $d$ , which appears in the expression for the phase found herein defined by Eq. (48). By comparing the equations for the phase, one can notice that the factor  $\frac{3}{2}$  occurs in Eq. (48), while in Eq. (91) it does not. This correction factor plays an important role in obtaining the accurate solution as illustrated in Fig. 11a, and, particularly, in Fig. 11b. Fig. 11b shows all these solutions for a longer period of time. The significant difference between the solution  $x^{yB}(t)$  and the exact one is seen, while the solution obtained herein  $x(t)$  defined by Eq. (90) agrees well with the numerical solution. Consequently, it is suggested that the phase of a pure-cubic oscillator should be calculated from Eq. (48) derived herein, instead of the expression given in [29,30].

## 5. Conclusions

In this paper, the oscillators with a non-negative real-power restoring force have been considered. The approximate solution for the motion of conservative oscillators has been expressed in the form of the Jacobi elliptic function. Its frequency has been obtained from the energy conservation law. The parameter of the elliptic function has been calculated by using Hamilton's variation principle and the stationary condition of the action integral. It has been shown that it has negative values when the power of the restoring force is less than unity and positive values when it is higher than unity. This solution has been used as a generating one for finding the motion of non-conservative oscillators. The equations for the amplitude and phase have been obtained by adjusting the Krylov-Bogoliubov method.

Unlike the existing techniques, the methods developed in this paper for conservative and non-conservative oscillators do not have any limitations regarding the value of the power of the nonlinear restoring force, which can have any non-negative real value. Their application is, thus, wider, and includes not only some generic nonlinear oscillators, such as the antisymmetric, pure quadratic or pure cubic oscillators, but also those with a non-integer-power restoring force. As expressed in the form of the Jacobi cn elliptic function, the solution for motion includes higher harmonics and has excellent accuracy with respect to the exact numerical solution.

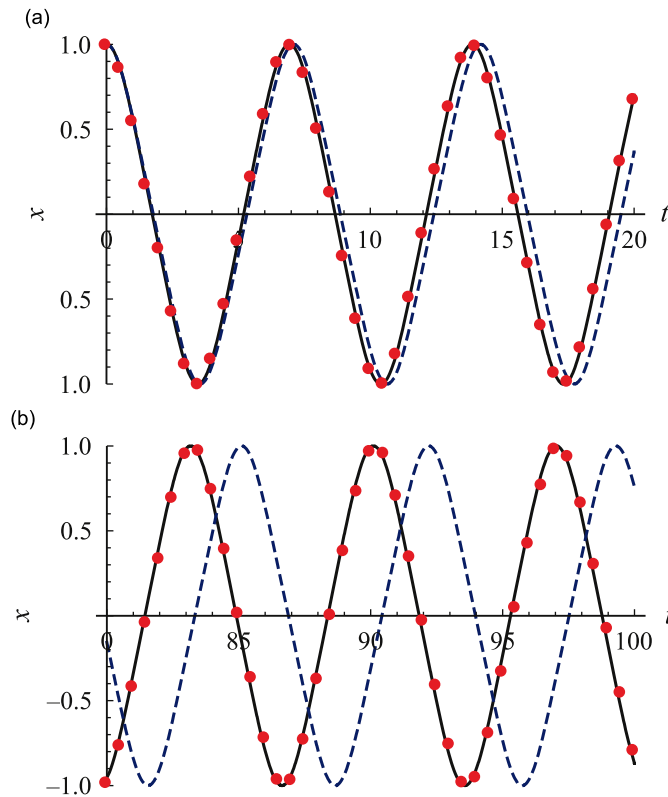


**Fig. 11.** Plots of the approximation given by Eq. (92) from [30] (dashed line) and the approximation given by Eq. (90) (circles) and the numerical solution of Eq. (89) (solid line) versus  $t$ : (a) at the beginning of motion and (b) after some longer period of time.

Several examples have demonstrated the applicability of the methods proposed to a wide range of oscillators with different powers of the restoring force and different forms of non-conservative forces. The amplitude and phase of the arbitrary-power oscillators with linear and viscous damping as well as with dry friction have been derived, which represent new results with research and reference values. The steady-state amplitude of the arbitrary-power oscillator with van der Pol damping is a new result, too. This amplitude has been calculated as the function of the power of the restoring force and has excellent accuracy. It has also been demonstrated that in comparison to the existing result for the phase of non-conservative pure cubic oscillators, the equation proposed here yields better results which are valid for longer time intervals. Hence, the improved version of this equation has been suggested.

## Acknowledgement

The research leading to these results has financially been supported by the Ministry of Science and Technological Development, Republic of Serbia (Project no. 144008).

## References

- [1] I. Kovacic, M.J. Brennan, T.P. Waters, A study of a non-linear vibration isolator with quasi-zero stiffness characteristic, *Journal of Sound and Vibration* 315 (2008) 700–711.
- [2] G. Gatti, I. Kovacic, M.J. Brennan, On the response of a harmonically excited two degree-of-freedom system consisting of linear and non-linear quasi-zero stiffness oscillators, *Journal of Sound and Vibration* 329 (2010) 823–1835.
- [3] P. Alabudzev, A. Gritchin, L. Kim, G. Migirenko, V. Chon, P. Stepanov, *Vibration Protecting and Measuring Systems with Quasi-Zero Stiffness*, Hemisphere Publishing, New York, 1989.
- [4] Z. Rakaric, Oscillator with a Fractional-order Restoring Force, MSc Thesis, University of Novi Sad, Faculty of Technical Sciences, Novi Sad, 2009 (in Serbian).
- [5] L. Cveticanin, M. Zukovic, Melnikov's criteria and chaos in systems with fractional order deflection, *Journal of Sound and Vibration* 326 (2009) 768–779.
- [6] D.M. Burns, V.M. Bright, Nonlinear flexures for stable deflection of an electrostatically actuated micromirror, *Proceedings of SPIE: Microelectronics Structures and MEMS for Optical Processing III*, Vol. 3226, September 1997, pp. 125–135.
- [7] C. Cortopassi, O. Englander, Nonlinear Springs for Increasing the Maximum Stable Deflection of MEMS Electrostatic Gap Closing Actuators, UC Berkeley <<http://www-bsac.eecs.berkeley.edu/~pister/245/project/CortopassiEnglander.pdf>>, accessed 28 July 2010.

- [8] Q. Zhu, M. Ishitoby, Chaos and bifurcations in a nonlinear vehicle model, *Journal of Sound and Vibration* 275 (2004) 1136–1146.
- [9] J.C. Dixon, *Tires, Suspension and Handling*, second ed., Society of Automotive Engineers, Warrendale, 1996.
- [10] M. Manciu, S. Sen, A.J. Hurd, Impulse propagation in dissipative and disordered chains with power-law repulsive potentials, *Physica D* 157 (2001) 226–240.
- [11] R.M. Rosenberg, The Ateb(h)-functions and their properties, *Quarterly Journal of Applied Mathematics* 21 (1963) 37–47.
- [12] R.E. Mickens, Oscillations in an  $\hat{x}(4/3)$  potential, *Journal of Sound and Vibration* 246 (2001) 375–378.
- [13] R.E. Mickens, Analysis of non-linear oscillators having non-polynomial elastic terms, *Journal of Sound and Vibration* 255 (2002) 789–792.
- [14] L. Cveticanin, Oscillator with fraction order restoring force, *Journal of Sound and Vibration* 320 (2009) 1064–1077.
- [15] I. Kovacic, Z. Rakaric, Oscillators with a fractional-order restoring force: higher-order approximations for motion via a modified Ritz method, *Communications in Nonlinear Science and Numerical Simulations* 15 (2010) 2651–2658.
- [16] P.G.D. Barkham, A.C. Soudack, An extension to the method of Krylov and Bogoliubov, *International Journal of Control* 10 (1969) 377–392.
- [17] R.H. Rand, Using computer algebra to handle elliptic functions in the method of averaging, A.K. Noor, L. Elishakoff, G. Hulbert (Eds.), *Symbolic Computations and their Impact on Mechanics*, Vol. 205, ASME PVP, New York, 1990, pp. 311–326.
- [18] V.T. Coppola, R.H. Rand, Averaging using elliptic functions: approximation of limit cycles, *Acta Mechanica* 81 (1990) 125–142.
- [19] M. Belhaq, F. Lakrad, On the elliptic harmonic balance method for mixed parity non-linear oscillator, *Journal of Sound and Vibration* 233 (2000) 935–937.
- [20] H. Hu, Exact solution of a quadratic nonlinear oscillator, *Journal of Sound and Vibration* 255 (2002) 789–792.
- [21] R.E. Mickens, *Truly Nonlinear Oscillations: Harmonic Balance, Parametric Expansions, Iteration, and Averaging Methods*, World Scientific, Singapore, 2010.
- [22] S.B. Waluya, W.T. van Horssen, On the periodic solutions of a generalized non-linear Van der Pol oscillator, *Journal of Sound and Vibration* 268 (2003) 209–215.
- [23] I.V. Andrianov, W.T. van Horssen, Analytical approximations of the period of a generalized nonlinear van der Pol oscillator, *Journal of Sound and Vibration* 295 (2006) 1099–1104.
- [24] S.H. Chen, X.M. Yang, Y.K. Cheung, Periodic solutions of strongly quadratic non-linear oscillators by the elliptic perturbation method, *Journal of Sound and Vibration* 212 (5) (1998) 771–780.
- [25] F. Lakrad, M. Belhaq, Periodic solutions of strongly non-linear oscillators by the multiple-scales method, *Journal of Sound and Vibration* 258 (4) (2002) 677–700.
- [26] S.H. Chen, X.M. Yang, Y.K. Cheung, Periodic solutions of strongly quadratic non-linear oscillators by the elliptic Lindstedt–Poincare method, *Journal of Sound and Vibration* 227 (5) (1999) 1109–1118.
- [27] S.H. Chen, Y.Y. Chen, K.Y. Sze, A hyperbolic perturbation method for determining homoclinic solution of certain strongly nonlinear autonomous oscillators, *Journal of Sound and Vibration* 322 (2009) 381–392.
- [28] S.B. Yuste, J.D. Bejarano, Construction of approximate analytical solutions to a new class of non-linear oscillator equations, *Journal of Sound and Vibration* 110 (2) (1986) 347–350.
- [29] S.B. Yuste, J.D. Bejarano, Improvement of a Krylov–Bogoliubov method that uses Jacobi elliptic functions, *Journal of Sound and Vibration* 139 (1) (1990) 151–163.
- [30] S.B. Yuste, Quasi-pure-cubic oscillators studied using a Krylov–Bogoliubov method, *Journal of Sound and Vibration* 158 (2) (1992) 267–275.
- [31] C.H. Yang, S.M. Zhu, S.H. Chen, A modified elliptic Lindstedt–Poincare method for certain strongly non-linear oscillators, *Journal of Sound and Vibration* 273 (5) (2004) 921–932.
- [32] H.P.W. Gottlieb, Frequencies of oscillators with fractional-power nonlinearities, *Journal of Sound and Vibration* 261 (2003) 557–566.
- [33] I.S. Gradshteyn, I.M. Ryzhik, *Tables of Integrals, Series and Products*, Academic Press, New York, 2000.
- [34] B. Vujanovic, S. Jones, *Variational Principles in Non-Conservative Phenomena*, Academic Press, Boston, 1989.
- [35] M. Abramowitz, I. Stegun, *Handbook of Mathematical Functions*, Dover Publications, New York, 1965.
- [36] N.I. Akhiezer, Elements of the Theory of Elliptic Functions, *Translations of Mathematical Monographs*, Vol. 79, American Mathematical Society, Providence, Rhode Island, 1990.
- [37] N.N. Bogoliubov, Y.A. Mitropolski, *Asymptotic Methods in the Theory of Non-Linear Vibrations*, Nauka, Moscow, 1974 (in Russian).
- [38] A.H. Nayfeh, D.T. Mook, *Nonlinear Oscillations*, Wiley, New York, 1979.
- [39] R.E. Mickens, *An Introduction to Nonlinear Oscillations*, Cambridge University Press, 1981.
- [40] P. Hagedorn, *Nonlinear Oscillations*, Clarendon Press, Oxford, 1981.